Advanced Diagnostics and Anomaly Detection for Railroad Safety Applications

Using a Wireless, IoT-Enabled Measurement System

Douglas L. Goodman, James Hofmeister, and Robert Wagoner

Ridgetop Group, Inc.
3580 West Ina Road
Tucson, AZ 85741, USA
doug.goodman@ridgetopgroup.com

Abstract—**Accidents involving trains have been attributed to degraded track and rolling stock. Detection of anomalies that indicate degraded condition is critical. In this paper we present results of an experiment using a sensor system mounted on one of the 110 boxcars on a train on a high-tonnage loop test track. The sensor was a microelectromechanical systems (MEMS) triaxial accelerometer module mounted on the hubs of the wheels of the boxcar. Sensor data were wirelessly transmitted to a collection gateway hub mounted inside the boxcar. The purpose of the experiment was to evaluate the feasibility of using a rotating triaxial accelerometer-based system designed to be mounted inside of a helicopter gearbox, and to use the system to detect anomalies in railroad tracks and rolling stock as well as anomalies of bearings, rotating shafts and gears. The results confirm it is feasible to identify, locate, and characterize such anomalies.**

Keywords—accelerometer; microelectromechanical; sensor; railroad track; boxcar; truck; axle; anomalies, IoT

I. Introduction

Sensors are at the heart of effective diagnostic measurement systems, and flexibility for integration into diverse platforms is required. Wireless internet technology, including Internet of Things (IoT), opens new avenues of supporting rigorous remote testing, diagnostic and prognostic systems. In a comprehensive prognostics and health management (PHM) system, sensor measurements are critical to providing the observability necessary to support the monitoring of spatially separated systems. Wireless technology supports selection of individual or multiple sensor input streams through a gateway collection hub where signal processing can be applied to the data stream to extract anomalies or degraded performance attributes; wireless technology enables use of unique IP addresses that can be interrogated for sensor measurements on an ongoing, near real-time basis; and standard wireless protocols can be used to feed sensor information from deep inside an enclosure such as a gearbox.

Collecting and processing measurement data is not straightforward because of many factors, including but not limited to noisiness of data from a sensor mounted on a boxcar axle, and the volume of digital data from high-bit resolution analog-to-digital data converters (ADCs). Wireless technology facilitates the transmission of digital data to a data-collection hub where a microprocessor transforms three-dimensional bit data into scalar data.

II. Setup: Test Train and Test Track

A. Mounting: Sensor System

A microelectromechanical systems (MEMS) based sensor module was mounted concentrically on the wheel hubs for each end of a boxcar axle of a train with 36-inch diameter wheels (see Fig. 1). The RotoSense™ module incorporates the MEMS sensor, wireless transmission, the PC board, receiving and storing data and data processing algorithms.

The MEMS device that was selected was configured for 3-axis coverage, 28 mV/g sensitivity, and a sample rate of 160 Hz. Analog data were digitized by three 16-bit ADC converters, stored in a local NVRAM, and then transmitted to a wireless network data-collection hub. This provides the net-centric bridge from low-power wireless mesh standard IEEE 802.11.4 protocol to the high bandwidth wired IEEE 802.3 standard, allowing connection to wireless switches and routers (see Fig. 2). The range of the wireless mesh transmission between collection hubs is approximately 10 meters/32 feet. The design includes the ability to collect data from a global positioning system (GPS) and store all the data remotely.

Fig. 1. RotoSense module mounted on the hub of a boxcar axle.

Fig. 2. Sentinel Gateway wireless data-collection hub.

B. Test Train and Track

The test train was about 1.3 miles in length, and comprised three locomotives and 110 boxcars. It was run on a high-tonnage loop (HTL) test track (see specs in Table I) for research under heavy axle-loads to test track-component reliability, wear, and fatigue. The test track is at the Transportation Technology Center in Colorado and is divided into test sections that generally correspond to tangents, spirals, curves, and turnouts that are populated with features and test sections (see Fig. 3). Examples of features are shown in Fig. 4, Fig. 5, Fig. 6, and Fig. 7.

After two laps, the train was auto-controlled to run at 40 mph: 15 four-minute laps of 2.67 miles each. On the fourth day, the train completed 132 laps. More than 14 billion digital bits were generated. The 16-bit outputs of each of the three ADCs split into two 8-bit nibbles and converted into two scalar values. Subsequent analysis and evaluation indicates that because of the noisiness of the data, it would be sufficient to use only the upper nibble.

TABLE I.   FEATURES OF THE HTL TEST TRACK

Test Track Feature		
# - Description	**# - Description**	**# - Description**
1 – lubricator	2 – steel bridge	3 – crib ties
4 – 405 turnout, frog	5 – thermite welds	6 – rail temperature test
7 – rail performance test	8 – concrete bridge	9 – LTM tests
10 – machine vision	11 – fiber optic cable	
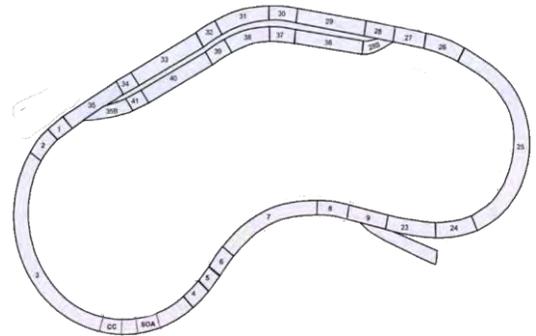
Fig. 3. Top view of the HTL test railway.

Fig. 4. Turnout and frog.

Fig. 5. Steel bridge.

Fig. 6. Concrete bridges.

Fig. 7. Crib ties (top); concrete bridges (bottom).

III. DATA ANALYSIS

A. Goal and Objectives of the Analysis

The goal of the analysis of the collected data was to prove the efficacy of RotoSense to detect high-force events (HFEs) that can be associated with features of interest (anomalies) on railroad tracks. HFEs that are not associated with known features can then be subjected to directed, focused inspection and investigation to discover damage requiring monitoring and/or maintenance.

The objectives of the data analysis are summarized as follows: (1) determine where in the data the train completes the two-lap test conditioning run (TCR); (2) determine a virtual origin for each lap of data to which HFEs can be referenced; (3) verify the speed of the train, the track length (a lap), and the distance traveled per sample; (4) select a threshold or thresholds to differentiate between HFEs and noise; (5) select a suitable number of laps of data to analyze; (6) create HFE patterns; (7) use pattern matching to associate HFE patterns to features such as those listed in Table I; (8) select pattern matches that exhibit an unambiguous relationship between an HFE and a test track (TT) feature; and (9) document the results. Fig. 8 is a block diagram of the analysis of sensor data.

B. Initial Train Movement

Fig. 9 is a plot of sensor data in the x-direction before and after the train begins to move. The pre-movement values for x, y, and z were calculated: x = 31,488; y = 32,768; and z =

32,768. These values were used to transform the sensor data to plus and minus values (see Fig. 10) to facilitate transforming the data into vectors.
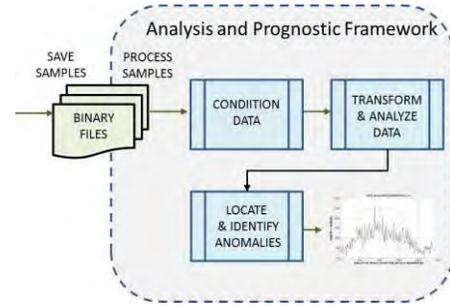
Fig. 8. Sensor, data collection, and post-processing diagram.
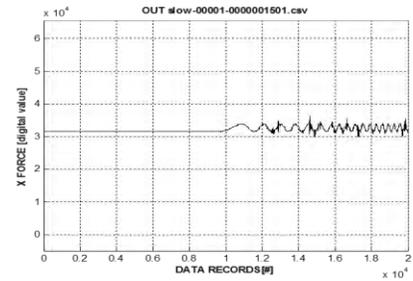
Fig. 9. Sensor data before and after train movement.
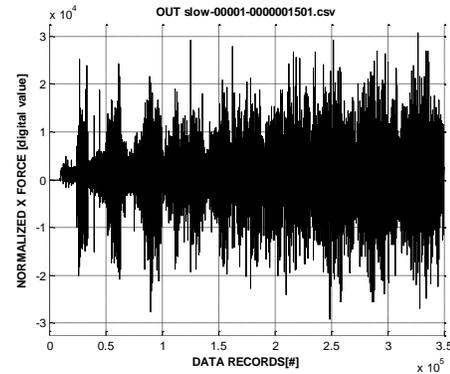
Fig. 10. Sensor data as the train comes to constant speed.

C. Train at Speed: Noise Suppression

After transforming the data into vectors using (1) and (2), various levels of noise suppression were used to condition the vector data. For example, Fig. 11 shows the result of using a noise margin (NM) of 25,000.[1]

$$XY = SQRT(x^2 + y^2) \qquad (1)$$

$$Z = SQRT(z^2) \qquad (2)$$

---

[1] Value of the digital bits of the sampled data.

D. Data Binning Based on Length of a Train Car

We concluded that we needed to bin the data because of the physical construction of boxcars: especially with respect to the use of two trucks per car, two axles per truck, and lack of cushioning between axles, between the axles and the trucks, and between the trucks and the bed of a boxcar (see Fig. 12).

- A force experienced by either wheel of a leading axle of a truck is transmitted to a sensor mounted on the hub of the trailing axle of the trailing truck.

- A track feature that causes a high-force event (HFE) results in as many as eight events being detected by the sensor.
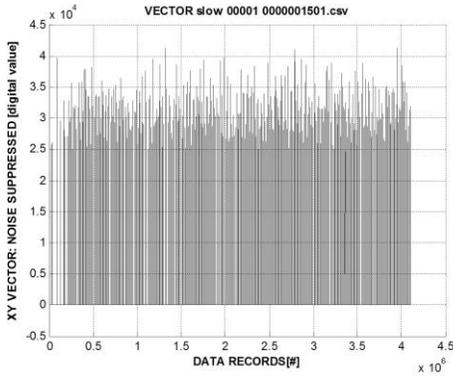
Fig. 11. XY vectors after noise suppression

Fig. 12. RotoSense sensor is mounted on the wheel of trailing axle of the trailing truck.

Although it is also likely that the mechanical coupling of boxcars causes transmission of HFEs from multiple boxcars, no attempt was made to characterize that effect.

Boxcars have lengths that vary from 50 feet to over 60 feet, with typical lengths of 58.5 to 60.5 feet, which led us to divide the 2.7 mile test track into 240 segments (bins) of 59.4 feet in length [1][2]. The result is summarized in Table II.

TABLE II.   Test Track Segments: Specifications

TT Length	Time per Lap	Time per Segment	Samples per Segment
14,256 feet	240 s	1 s	160

E. Data Analysis: Binned Data Method

Fig. 13 is an example of binned data for all 240 segments after suppressing all data using NM = 25,000. The plotted bin counts and pattern matching results are shown in Fig. 14, Fig. 15, and Fig. 16. Table III tabulates the TT segments, the corresponding TT IDs, the track features, and whether the feature was detected.
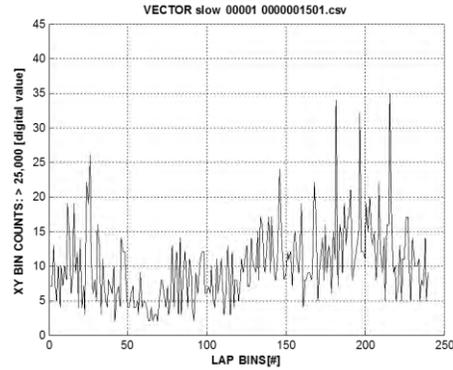
Fig. 13. XY bin counts after noise suppressed.

TABLE III.   Test Track: Sections, ID, Feature, and Status

Track Sections	Track ID	Track Feature	Detected
1 – 3	S1	Lubricator	
4 – 5	S2		
5 – 26	S3	Repair/overlay welds	Yes
30 – 40	S3	Concrete bridges	Yes
42 – 46	S3	Concrete bridges	Yes
63 – 66	S4	Steel bridges	
67 – 69	S5	Bridge deflection	
70 – 73	S6	Steel bridges	
74 – 92	S7	Rail performance	
93 – 97	S8	Fiber optic cable	
98 – 108	S9	405 turnout and frog	Yes
109 – 117	S23	405 turnout and frog	Yes
118 – 125	S24	Lubricator	
126 – 163	S25	TPO, tie & fastener	Yes
164 – 170	S26		
171 – 175	S27	Lubricator	
176 – 180	S28	Turnout – foundation	Yes

Track Sections	Track ID	Track Feature	Detected
181 – 193	S29	LTM tests	
194 – 198	S30		
199 – 208	S31	FRA: rail-seat deterioration Thermite welds	Yes
209 – 212	S32		
213 – 225	S33	Crib ties	Yes
226 – 229	S34		
230 – 240	S35	407 turnout	Yes
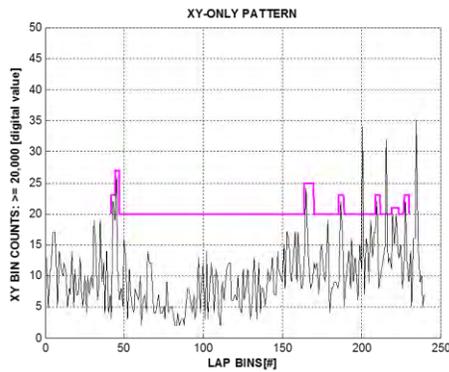
Fig. 14. XY bin counts and pattern matching.
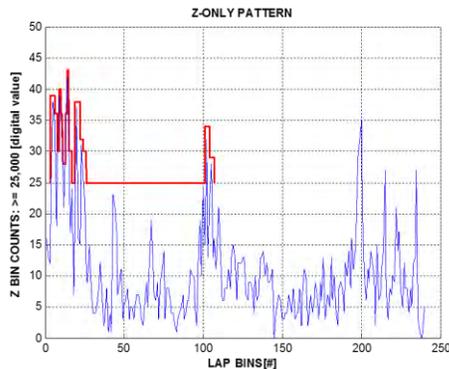
Fig. 15. Z bin counts and pattern matching.
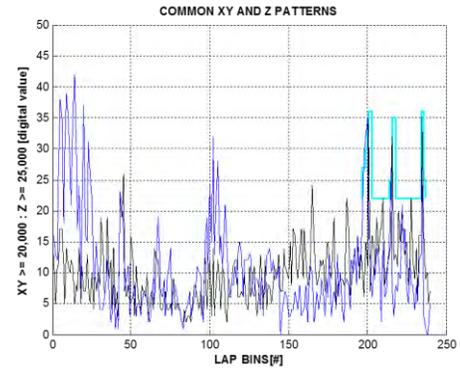
Fig. 16. XY and Z bin counts and common pattern matching.

IV. BINNING AND PATTERN-MATCHING RESULTS

The results of pattern matching using binned data are seen in Fig. 17. The eight circled counts were matched to 10 track features/anomalies as listed in Fig. 18 and tabulated in Table III. In spite of the noisiness of the data, and the likelihood of "jitter" in the data, the results are excellent. We met our goal: "The goal of the analysis of the collected data was to prove the efficacy of RotoSense to detect high-force events (HFEs) that can be associated with features of interest (anomalies) on railroad tracks."
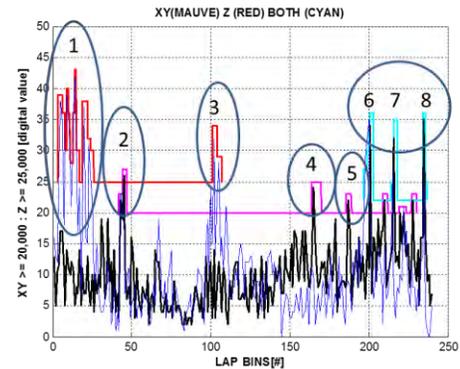
Fig. 17. Composite bin counts and pattern matching.

1. Repair/overlay welds, concrete bridge
2. Concrete bridge
3. 405 turnout and frog
4. TPO, ties and fastener, performance
5. Turnout, steering switch, foundation
6. FRA, rail-set deterioration, welds
7. Crib ties
8. 407 turnout

Fig. 18. Track features (anomalies) matched to binned data.

V. IMPROVED FILTERING

An important objective of the data analysis was to show that even without GPS, the captured RotoSense data could be used to identify and locate significant railway features/anomalies such as turnouts. Examination and

comparison of Fig. 17, Fig. 18, and Table III provides evidence the objective is met; however, the data are noisy.

A. Particle Filtering

The physical structure of the boxcar on which RotoSense was mounted to the wheel hubs results in the detection of a multiplicity of anomalies. Processing of signals from all wheel hubs can help pinpoint the sources of anomalies such as cracked rails or wheels, broken welds, or other worn components. The HFEs that are detected during the time it takes the boxcar to traverse a point on the track can be averaged: All HFEs that occur in a track segment can be classified as caused by a single feature.

B. FilteringResults

For four laps, a single HFE location was detected (see Fig. 19); after 13 laps a total of five HFE locations were detected – there was no discernible change in the amplitude of the average HFE at that location (Fig. 20); and after 20 laps, there were six locations (see Fig. 21).
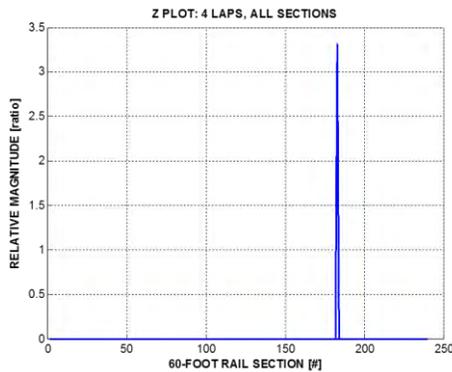
Fig. 19. Single HFE location is detected in four laps of 240 segments.
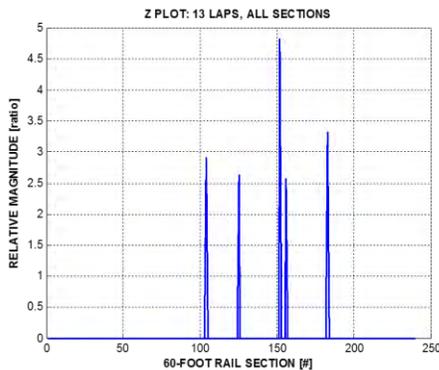
Fig. 20. Five HFE locations are detected in 13 laps of 240 segments.
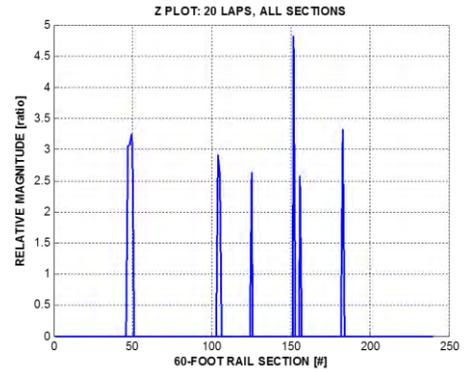
Fig. 21. Six HFE locations are detected in 20 laps of 240 segments.

VI. PHM MODELING: PREDICTIVE

Advanced prognostics in condition-based data (CBD) systems uses methods such the following:

- Detect the onset of degradation, and use a predictive model to predict a future time of failure.

- Monitor the degraded unit and measure the rate of change in degradation, use the rate to adjust a predictive model, and use the adjusted predictive model to predict a new future time of failure.

As railways degrade, increasing degradation is likely to be manifested as an increasing force experienced by the wheels of the train cars. Therefore there are at least two candidates for fault-to-failure progression (FFP) signatures: increase in the number of HFEs and increase in the HFE magnitude as degradation increases.

The predictive algorithms process both linear and nonlinear signature data: the algorithms use Kalman-like filtering methods; the algorithms are not computationally intensive; and the algorithms are fast and accurate:

- Converges to within 25% of true end of life (TEOL) with an average of more than 80% remaining functional life.

- Converges to within 10% of TEOL with an average of more than 70% remaining functional life.

- Converges to within 5% of TEOL with an average of more than 50% remaining functional life.

- Produces in near real time:
  - o estimates of remaining useful life (RUL)
  - o estimates of state of health (SoH)
  - o estimates of prognostic horizon (PH)

VII. RECOMMENDATIONS

During analysis, the following were noted:

- The sensitivity of the sensor can benefit from calibrating to the train speed.

- The sampling rate of the sensor assembly should be increased to at least 14 kHz to detect narrower gaps. At 160 samples per second and a train speed of 40 mph, the train will travel 704 inches per second, which means if it is desired to reliably detect a one-inch gap, the sensor needs to sample at least once every 0.5 inch.

VIII. SUMMARY AND CONCLUSIONS

The sampling rate of the sensor assembly should be increased to at least 14 kHz to detect narrower gaps. At 160 samples per second and a train speed of 40 mph, the train will travel 704 inches per second. For a 0.5 inch gap in the rail, one sample per 0.5 inch is desirableSummary and Conclusions

In this paper we presented the results of a test configuration using a sensor system mounted on one of the 110 boxcars on a train on a high-tonnage loop test track..

The purpose of the experiment was to evaluate the feasibility of using the system to detect anomalies in railroad tracks and rolling stock. The results confirm it is feasible to detect, identify, locate, and characterize such anomalies.

- Ten locations (out of 14) were detected.

- Both binning and particle-based methods of conditioning data were used.

- Two fault-to-failure progression signature candidates are identified.

- A predictive processor using extended Kalman-like filtering (EKF) already exists and has proven to work on more than a dozen different devices and units.

- Further work will include adjusting RotoSense for increased dynamic range and accuracy, as well as interfacing to downstream digital signal processing as part of a more comprehensive analysis system.

ACKNOWLEDGMENT

REFERENCES

[1] "Railroad Equipment, 50' Standard Boxcar," CSX de Mexico, www/csx.com, accessed 9/4/2015.

[2] BOX CAR 50 FT/ 286 GRL, BNSF 728400 – 728999, BNSF Railway, pp. 135-1, 7/16/2008.

[3] E. Orhan, "Particle Filtering," Center for Neural Science, University of Rochester, Rochester, NY, 8/11/2012.

[4] A. Doucet and A. Johansen, "A Tutorial on Particle Filtering and Smoothing: Fifteen Years Later," Institute of Statistical Mathematics, Tokyo, Japan, University of Warwick, Coventry, UK, 12/19/2008.

[5] G. Terejanu, "Extended Kalman Filter Tutorial," University at Buffalo, Buffalo, NY, 5/18/2008.